Published in IET Optoelectronics as an invited paper
Received on 7th July 2008
doi: 10.1049/iet-opt.2008.0038

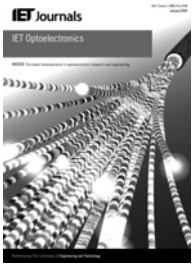

ISSN 1751-8768

Modelocked integrated external-cavity surface emitting laser

A.-R. Bellancourt D.J.H.C. Maas B. Rudin M. Golling T. Südmeyer U. Keller

Department of Physics, Institute of Quantum Electronics, ETH Zurich, Wolfgang-Pauli-Str. 16, 8093 Zurich, Switzerland
E-mail: bellancourt@phys.ethz.ch

Abstract: A modelocked integrated external-cavity surface emitting laser (MIXSEL) is a novel type of ultrafast semiconductor laser that integrates a saturable absorber directly into a vertical external cavity surface-emitting laser. The saturable absorber requirements and integration challenges to obtain self-starting and stable pulse formation are discussed. One single quantum dot absorber layer was optimised for this application. Since the first feasibility demonstration of an optically pumped MIXSEL, the authors have further improved the average output power to 185 mW with 32 ps pulses at around 3 GHz pulse repetition rate at a centre wavelength of $\simeq$957 nm. The authors analyse and discuss the challenges for further power scaling and pulse shortening. The MIXSEL concept appears suitable for cost-efficient wafer-scale mass production when the external cavity is defined by a transparent wafer into which the curved output coupler can be etched. The semiconductor MIXSEL structure would then be glued to such a transparent wafer. The potential for electrically pumped MIXSELs will make this laser technology even more attractive.

1 Introduction

Diode-pumped picoseconds and femtosecond solid-state lasers have made a large impact since the early 90s in both fundamental science and industrial applications [1]. However, so far, ultrafast lasers have not achieved the impact of continuous-wave (cw) lasers, which are used in various everyday life applications, such as compact disk players, optical communication or laser printers. One reason for this lower market penetration is the complexity and cost of these sources. Even in long distance fibre-optic communication with light pulses, modelocked semiconductor lasers are currently not used in commercial systems. Instead a cw laser is typically applied with external modulators that first carve the pulses and then modulate the information onto the data stream. However, future telecom transmission systems at 10 Gb/s and higher will benefit from modelocked lasers for return-to-zero formats [2] and soliton dispersion management techniques [3].

In recent years, scaling up the processing power of microprocessors with ever increasing clock rates has hit a plateau. To continue ramping up performance according to the expectations of Moore's law, companies such as Intel and AMD have turned to multi-core processing [4]. In order to increase performance and save energy, most future processor chips will contain many if not hundreds of smaller processors, so-called cores, that work in parallel. As a consequence, almost all software must exploit parallelism and the cores need to be interconnected at the full clock rate. This multi-core revolution will cause a paradigm shift in computer science and will push forward the impact of optics from long-distance communication to optical clocking inside such multi-core processors. This is where a cw modelocked laser, that is, a very stable optical pulse generator can provide a stable external clock, which can be easily distributed to all cores. For this application, an ultrafast laser technology will most likely need to provide a pulse repetition rate ranging from a few GHz to 100 GHz to define a road map, and an average output power of more than 100 mW (depending ultimately on the number of cores) with pulse durations in the few picosecond regime.

Compact and reliable ultrafast lasers are also important for application areas as diverse as biology, medicine or metrology.

Ultrafast lasers enable supercontinuum generation in optical fibres, which is important for applications in microscopy and imaging. For example, optical coherence tomography can provide high-resolution two- and three-dimensional images of biological tissue in a fast, non-invasive way [5, 6]. Furthermore, the high peak power of femtosecond lasers can enable nonlinear optical processes for multi-photon and fluorescence imaging [7], which enables high-resolution microscopy of biological samples. Frequency combs generated by femtosecond pulses enable high-precision metrology [8], which significantly can improve the accuracy of clocks [9–11]. For example, more reliable and compact ultrafast laser systems are needed to enable space-based devices for future global positioning systems.

Semiconductor lasers are based on the most promising technology to enable cost-efficient mass production of reliable ultrafast lasers. Semiconductor bandgap engineering gives much more freedom to design the laser for wavelength regions that are not covered by established solid-state laser gain materials. Current ultrafast edge emitter lasers seem to have many trade-offs for the above-mentioned applications because of their transverse beam quality, limited output power and pulse repetition rate scaling. An interesting alternative is the vertical external cavity surface-emitting laser (VECSEL) [12], which combines the benefits of semiconductor and diode-pumped solid-state lasers. VECSELs typically operate in the visible red and mid-infrared [13] spectral regions, but they also can generate blue and ultraviolet light by efficient intracavity frequency doubling [14]. Vertical propagation of the laser light perpendicular to the epitaxial layers of the semiconductor structure has several advantages compared with edge-emitting lasers, where the laser beam propagates along the epitaxial layers. The vertical geometry avoids facet damage even for multi-watt output power levels by simply scaling the mode area with power. This is very simple for optical pumping but more challenging for electrical pumping [15]. But even with electrically pumped VECSELs power as high as 0.5 W has been demonstrated [16]. For optically pumped (OP) VECSELs, the output power can be scaled up with the pump power just by increasing the pump spot diameter on the VECSEL. Similar to solid-state lasers, the external cavity and mode-matched optical pumping results in high efficiency, high power and excellent transversal mode quality. Average cw output powers of up to 30 W with an M^2 of 3 [17], and 20 W with an M^2 of <1.1 [18] have been reported from OP-VECSELs.

VECSELs can be modelocked with an intracavity saturable absorber [19]: self-starting ultrafast pulse formation is usually achieved with a semiconductor saturable absorber mirror (SESAM) [20]. To date, this SESAM-VECSEL modelocking approach resulted in high average power levels (up to 2.1 W average power in 4.7 ps pulses), short pulse durations (100 mW in 477 fs pulses [21] or 290 fs pulses with 10 mW [22]), and high repetition rates (50 GHz with 102 mW in 3 ps pulses) [23]. Such performance is attractive for many applications, however, the complexity of these lasers is still too high for mass production: two separate semiconductor elements need to be combined in a folded cavity (V-cavity) [23].

Recently, we have successfully demonstrated SESAM integration into the VECSEL gain structure and achieved stable modelocking with 40 mW average output power [24]. Modelocking was achieved from a simple, straight cavity, with the potential for wafer scale integration and adjustable repetition rates. We refer to this class of devices as the modelocked integrated external-cavity surface emitting laser (MIXSEL). The MIXSEL platform has a large potential for all mentioned applications. For example for optical clocking of multi-core microprocessors, it should be possible to define a road map for a pulse repetition rate up to $\simeq$100 GHz. The vertical MIXSEL geometry in comparison to the edge-emitting semiconductor laser has the advantage that undesirable nonlinear interactions that tend to distort the pulses and destabilise modelocking are strongly limited, because the interaction length with the semiconductor gain medium is very short. For example at 50 GHz the optical cavity length is 3 mm, the semiconductor structure only adds about 10 μm to the cavity length and most of the beam will propagate in air or a transparent wafer. Therefore changing the pulse repetition rate mainly requires a change in the propagation length in the fully transparent section without substantially changing the physical dynamics of the laser.

In this paper, we review in more detail the key achievements that permitted the transition from the SESAM-VECSEL to the MIXSEL approach. We start with a discussion on the VECSEL gain structure and the requirements for stable pulse formation, which led to the development of a specialised quantum-dot absorber. Afterwards, we focus on the MIXSEL design and the integration challenges. We then discuss thermal limitations and power scaling possibilities. Finally, we present a MIXSEL that generates five times higher output power than previously obtained [24] but is still thermally limited by its remaining GaAs substrate (i.e. 'right-side-up' structure as discussed later).

2 Moving from the SESAM-VECSEL to the MIXSEL approach

A VECSEL consists of an OP semiconductor gain structure and an external resonator (Fig. 1*a*). VECSEL gain structures are usually grown by molecular beam epitaxy (MBE) or metalorganic vapour phase epitaxy using various semiconductor materials. Our structures were grown with an MBE on 600 μm thick GaAs (100) substrates. We designed our gain structures for an emission wavelength around 960 nm and a pump wavelength of 808 nm. The pump radiation is applied at an angle of 45°. Our VECSEL epitaxial structure (Fig. 1*b*) consists of a double periodic distributed Bragg reflector (DBR) to reflect both the laser and pump wavelengths; a gain section composed of seven

doi: 10.1049/iet-opt.2008.0038

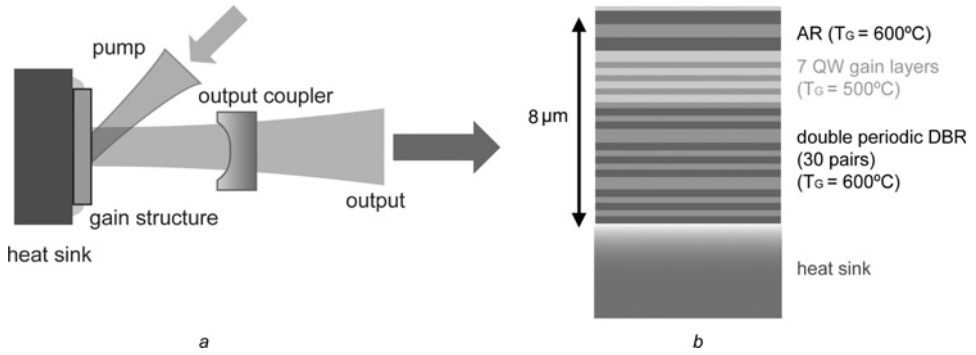

Figure 1 *OP VECSEL and its layer structure*

a OP VECSEL
The VECSEL gain structure is soldered to a heat sink and OP at 808 nm at an angle of incidence of ≃45°
b VECSEL layer structure: DBR, AR, QW

InGaAs quantum wells (QWs) embedded in GaAs layers that absorb the pump light, and an antireflection (AR) coating on top. The DBR and AR coating are grown around 600°C whereas the active region is grown at 500°C. The layer structure thickness is around 8 μm, which corresponds to about 20 h of growth time in the MBE.

The vertical emission of VECSELs enables both high average power and excellent transverse beam quality. The output power can be scaled up simply by increasing both the pump spot diameter and the pump power, if the heat flow through the layer structure is nearly one-dimensional [25]. This is unfortunately not the case if the gain structure is grown on top of a 600 μm thick GaAs substrate. The relatively low thermal conductivity of 46 W/mK for GaAs is significantly lower than for copper (390 W/mK) or diamond (2000 W/mK). Efficient heat removal can be realised by bonding a transparent material with higher thermal conductivity on top of the gain structure (typically diamond) [26]. However, such a heat spreader can introduce thermal lensing and aberrations or unwanted etalon effects with strongly increased dispersion. Another option is to completely remove the GaAs substrate. The semiconductor structure is only a few microns thick and cannot be handled without support. Growing the structure in reverse order (so-called 'upside-down' structure) enables to solder the structure to a heat sink and to remove the substrate. This method requires several processing steps. After the growth of the etch stop layer and the upside-down gain structure, the wafer is metallised and soldered in vacuum onto a copper or diamond heat sink. Then the substrate is mechanically thinned down and etched away. The remaining semiconductor structure thickness is <10 μm, which is smaller than the pump spot (>100 μm diameter), and the resulting one-dimensional heat flow allows to scale up the output power by increasing the pump power without increasing the temperature gradient [25].

Passive modelocking is achieved with an intracavity SESAM [20], which initiates and stabilises pulse formation. The SESAM is used as an end mirror in the cavity. A SESAM consists of a DBR and an absorber layer (Fig. 2*a*). The saturable absorber layer can be a bulk, a QW or a quantum dot (QD) layer. The reflectivity of the SESAM increases with pulse fluence (Fig. 2*b*). The total change of reflectivity is referred to as the modulation depth (ΔR), whereas the constant loss, because of scattering or point defects, is referred to as the non-saturable loss (ΔR_{ns}.). Our SESAMs are grown by MBE on a GaAs substrate. The DBR is grown at high temperature (~600°C) for minimum defect densities and low scattering losses, and the absorber layer is typically grown at lower temperature for higher

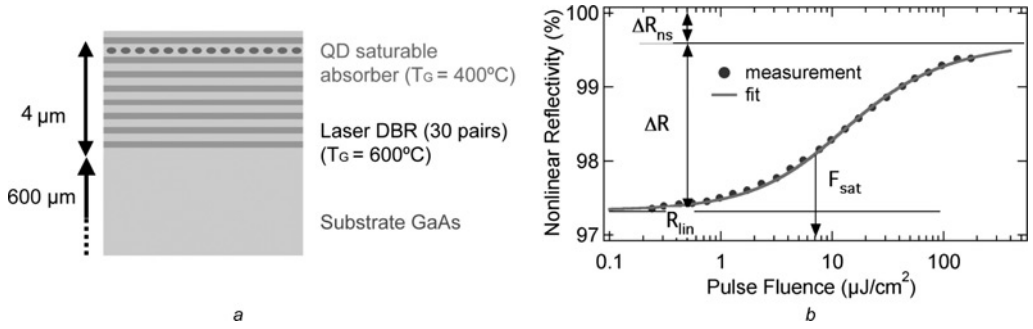

Figure 2 *QD-SESAM layer structure and nonlinear reflectivity*

a QD-SESAM layer structure
b Measured nonlinear reflectivity [28] of a QD-SESAM grown at 430°C and annealed for 4 h at 600°C in the MBE

defect density, that act as traps for faster recombination [27]. In case of QD-SESAMs, we have grown the QD layer and its surrounding GaAs cap layer around 350–400°C. For SESAM-VECSEL modelocking, typical modulation depths are between 1 and 5%, and the non-saturable loss should be below 0.5%.

An important parameter for achieving stable modelocking is the saturation fluence (F_{sat}) [29, 30] (Fig. 2*b*). In contrast to solid-state lasers, the gain in a semiconductor VECSEL exhibits dynamic gain saturation. In order to form a short net gain time window for stable pulse formation, the saturation of the absorber needs to be faster and stronger than the gain saturation (Fig. 3*a*) [31]. The condition for achieving stable modelocking is

$$\frac{E_{sat,a}}{E_{sat,g}} = \frac{F_{sat,a}A_a}{F_{sat,g}A_g} \ll 1 \qquad (1)$$

where $E_{sat,a}$ is the saturation energy of the absorber and $E_{sat,g}$ of the gain; $F_{sat,a}$ is the saturation fluence of the absorber, $F_{sat,g}$ of the gain; and A_a and A_g the cavity mode area in the absorber and the gain, respectively. As can be seen from (1) modelocking can be achieved either by significantly reducing the laser mode area on the SESAM (by focusing onto the SESAM); or by choosing a saturable absorber with lower saturation fluence. Typical QW-SESAM show a similar saturation fluence than the QWs used in the gain region, and stable pulse formation is usually achieved by strong focusing onto the QW-SESAM (10–40 times smaller area than in the gain) (Fig. 4*a*).

In a MIXSEL we cannot apply stable modelocking with stronger focusing inside the absorber layer (Fig. 4*a*) because the beam diameters in the absorber section and the gain section are about the same. The saturable absorber and the gain are both integrated in the semiconductor MIXSEL structure, which is much shorter than the total external cavity length in the multi-10 GHz regime, and therefore lies well within the depth of focus of the cavity mode (Fig. 4*c*). Therefore saturable absorbers with lower saturation fluence than our standard QW-SESAMs are required to obtain modelocking with the same laser mode areas in the absorber and the gain (Fig. 4*b*). The saturation fluence of a SESAM can be reduced by increasing the electric field strength in the absorber with a more resonant design [32]. However, in the case of our standard QW-SESAM, this would increase the modulation depth to values above 5%, which is too large for stable modelocking. Therefore standard QW saturable absorbers appear unsuitable for an integrated structure. The key solution to resolve the saturation issue and achieve modelocking with identical spot sizes in a 1 : 1 modelocking approach was the development of QD saturable absorbers.

QDs have been extensively used for as a gain medium for edge-emitting lasers [33] and more recently for vertical-emitting lasers [34]. Multi-layer QD-SESAMs have been developed to modelock VECSELs [35] and diode-pumped solid-state lasers [23, 36]. Edge-emitting QD lasers exhibit a number of compelling advantages, such as a large wavelength tunability thanks to the wide spectral gain, a lower threshold and lower temperature sensitivity [37]. With the additional parameter of the dot density, we were able to obtain both low saturation fluence in a more resonant SESAM design and a reasonably small modulation depth – an achievement that was not possible with QW-SESAMs. With a more resonant SESAM design, we can enhance the field strength in the absorber section and reduce the aturation fluence, that, however, also increases the modulation depth. With QD-SESAMs we could reduce the modulation depth again with a lower QD density. A single layer QD SESAM enabled the first 1 : 1 modelocking of a VECSEL [38] (Fig. 4*b*). Elimination of the focusing constraint enabled shorter cavity geometries with up to 50 GHz repetition rates because the VECSEL-SESAM structure distance as shown in Fig. 4*b* could be reduced [39]. Moreover, with the successful 1 : 1 modelocking demonstration the integration of the absorber in the VECSEL structure became conceptually possible. Fig. 4 illustrates the evolution from modelocked VECSELs with a QW-SESAM, 1 : 1 modelocking using a QD-SESAM, and the integration of the QD absorber into the VECSEL epitaxial structure – referred to as the MIXSEL.

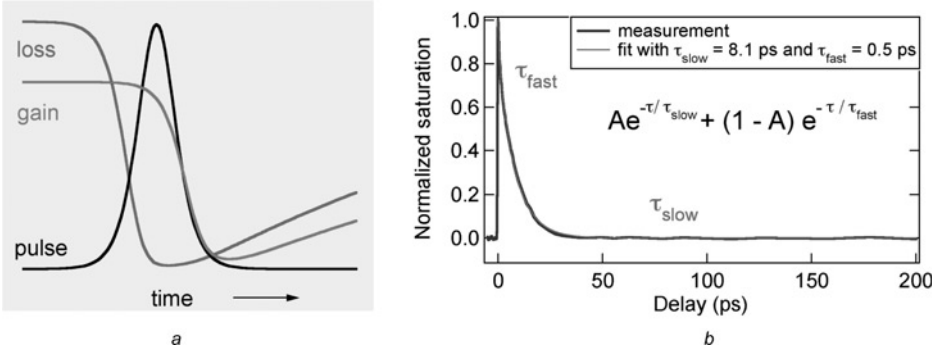

Figure 3 *SESAM modelocking principle and recovery*

a Passive modelocking with slow saturable absorber and dynamic gain saturation
b Pump probe measurement of a typical QD-SESAM

IET Optoelectron., 2009, Vol. 3, Iss. 2, pp. 61–72
doi: 10.1049/iet-opt.2008.0038

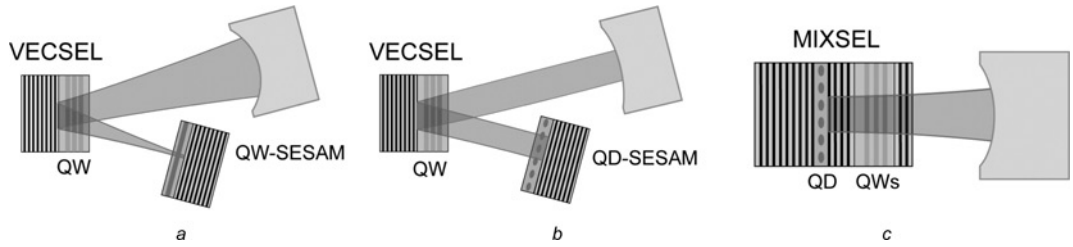

Figure 4 *From VECSEL to MIXSEL*

a Folded-cavity with focusing onto the QW-SESAM
b Folded-cavity with the same beam radius on VECSEL and QD-SESAM (i.e. 1 : 1 modelocking)
c Straight cavity of the MIXSEL with the integrated QD absorber and the QW gain

3 MIXSEL design and integration challenges

A typical MIXSEL semiconductor structure (Fig. 5) contains two DBRs: one for the laser wavelength and one for the pump wavelength with the absorber layer embedded in between. The laser DBR, high reflecting at 960 nm, consists of 30 pairs of AlAs/GaAs layers. In order to prevent the pump light from bleaching the saturable absorption of the QD layer, the pump DBR is highly reflective for the 808 nm pump, but highly transmissive for the 960 nm laser light. It is composed of AlAs and $Al_{0.2}Ga_{0.8}As$, which do not absorb the pump light. The InAs QD absorber layer is made of self-assembled InAs QDs and capped with low-temperature GaAs layer to freeze the QDs' shape (Fig. 6). The gain region is located on top of the pump DBR and consists of seven 8 μm thick $In_{0.13}Ga_{0.87}As$ QWs placed in an antinode of the electric field. The layer structure is covered by an AR coating.

Combining two different elements, the VECSEL gain structure optimised for high gain, and the QD-SESAM optimised for low saturable saturation fluence and fast recovery, raises several challenges. Different growth temperatures are used for different layers leading to annealing and material quality issues. The low-temperature grown QD layer is located between two high-temperature grown DBRs. The electric field strength in the QD absorber is enhanced by a more resonant design to reduce the saturation fluence (see previous section), but also increases the sensitivity towards growth errors.

For the initial proof-of-principle demonstration, we grew the MIXSEL on a 600 μm thick GaAs substrate without any substrate removal. This is the 'right-side-up' MIXSEL because the epitaxial growth is not done in reverse order as discussed above. The low-thermal conductivity through the thick GaAs substrate limits the achievable output power, but in contrast to the previously discussed 'upside-down' growth, no further wafer processing is required. This enables a faster turn-around for testing and optimisation to address the various growth issues.

3.1 QDs growth

A low-temperature QD absorber integrated in the middle of the MIXSEL structure is exposed to long annealing times during the continuation of the growth and may introduce defects for the gain section of the MIXSEL. This is more severe for the 'right-side-up' MIXSEL because the QD absorber is grown before the gain. In this case the intermediate DBR helps to clean up any defects introduced by the QD growth. The defect issue should be less severe for the 'upside-down' MIXSEL for which the gain is grown before the absorber.

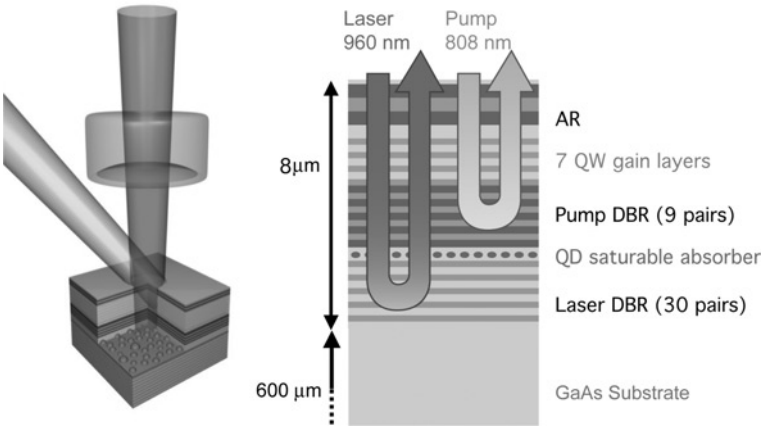

Figure 5 *MIXSEL design and schematic layer structure*

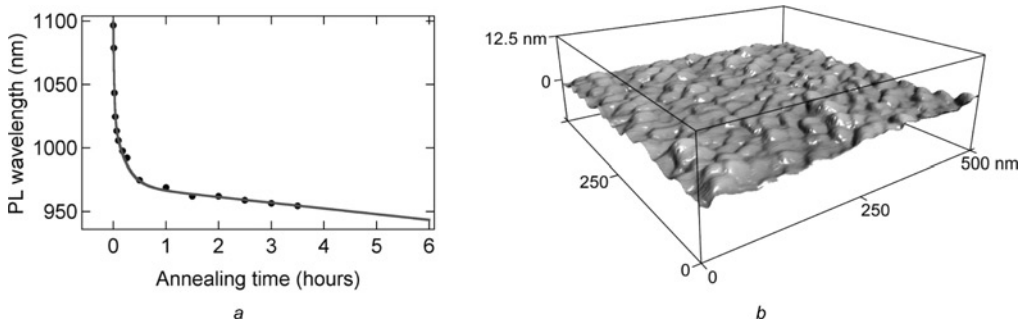

Figure 6 *QDs annealing and atomic force microscopy (AFM) image of QDs*

a Blueshift of the photoluminescence centre wavelength of QD test structure (QDs grown at 400°C) as a function of annealing time at 600°C

b Atomic force microscopy image of QDs grown at 430°C (without annealing)

The number of defects in the MIXSEL gain section has to be minimised and therefore we had to optimise the QD saturable absorber parameters under full integration conditions. The main growth parameters that will influence the QDs shape and properties are the in-content, measured in monolayers, the growth temperature and the annealing time and temperature. The QD layer in the QD-SESAMs used for 1 : 1 modelocking in references [38, 39] was grown at temperatures around 350°C in order to achieve sufficiently fast recovery time. For the first 1 : 1 modelocking demonstration, the resonant SESAM had a modulation depth of 3%, non-saturable losses of 0.3% and a saturation fluence of 1.7 $\mu J/cm^2$ [38]. However, first MIXSEL integration tests showed that such a low-temperature grown QD-layer would introduce too many defects in the subsequently grown layers. Increasing the growth temperature of the QD layer reduces the defect density and improves the material quality of the surrounding layers. But it also affects the absorption parameters such as the modulation depth and recombination time of the QD absorber. A compromise between good material quality for high lasing efficiency (higher temperature) and fast recovery time and optimum saturation fluence (lower temperature) was found with a growth temperature of 430°C. Increasing the temperature further led to higher gain, but the saturable absorption at our laser wavelength became too low for stable modelocking.

It is important for the QD absorber design to take into account the annealing effects on the QDs during the subsequent growth at higher temperature. This annealing modifies the dot composition and size [40] resulting in a blue shift of the absorption and emission wavelength of about 100 nm for a few hours at 600°C. We measured the wavelength shift with annealing studies of QD test structures. We annealed different samples at varying temperatures and durations with rapid thermal annealing (RTA). The evaporation of the arsenic during the annealing process was prevented with a SiOx-coating using plasma-enhanced chemical vapour deposition. After RTA these protective coatings have been removed by etching. As shown in Fig. 6*a* the main change of the QD properties occurs during the first hour and can easily be observed by a strong wavelength shift of the photoluminescence spectra. We could accommodate for this blue shift by adapting the QD growth parameters to a photoluminescence peak at 1100 nm before annealing. After the MIXSEL growth, the QD photoluminescence was shifted by annealing to ≃950 nm matching our lasing operation wavelength. In Fig. 2*b*, the measured nonlinear reflectivity curve of a QD-SESAM grown on the same conditions as the MIXSEL is shown. It was grown at 430°C and annealed at 600°C for about 4 h in the MBE. We measured a saturation fluence of 7 $\mu J/cm^2$, a modulation depth of 2.3% and non-saturable loss of 0.4%. The measurement set-up is described in [28].

3.2 Field enhancement and dispersion

For optimised absorber saturation we need to design and control the laser field enhancement in the gain and the absorber layers. The saturation fluence can be reduced with an increased field strength in the absorber by introducing an intermediate mirror between the QD layer and the pump mirror (Fig. 7 top). The number of layers in the intermediate DBR mirror determines the enhancement factor. In Fig. 7, we compare the simulated field intensity of our MIXSEL design, which contains a five-pair intermediate DBR, with a MIXSEL containing a one-pair intermediate DBR. The higher field strength in the QD-layer with a higher resonance reduces the saturation fluence by a factor of four. The seven QW gain layers are placed in different antinodes of the electric field. Increasing the field strength in the QW-antinodes would lead to higher gain but would also tend to destabilise passive modelocking.

The growth error sensitivity of an integrated MIXSEL structure is higher than for separate VECSEL and SESAM, since both electric field enhancements and dispersion depend critically on layer thicknesses and layer material composition. For example, an increase of 1% on the AlAs thickness would, at a fix wavelength, increase the relative field intensity in the absorber from 4.4 to 7.1 and decrease the field intensity in the QWs from 1.067 to 0.88.

doi: 10.1049/iet-opt.2008.0038

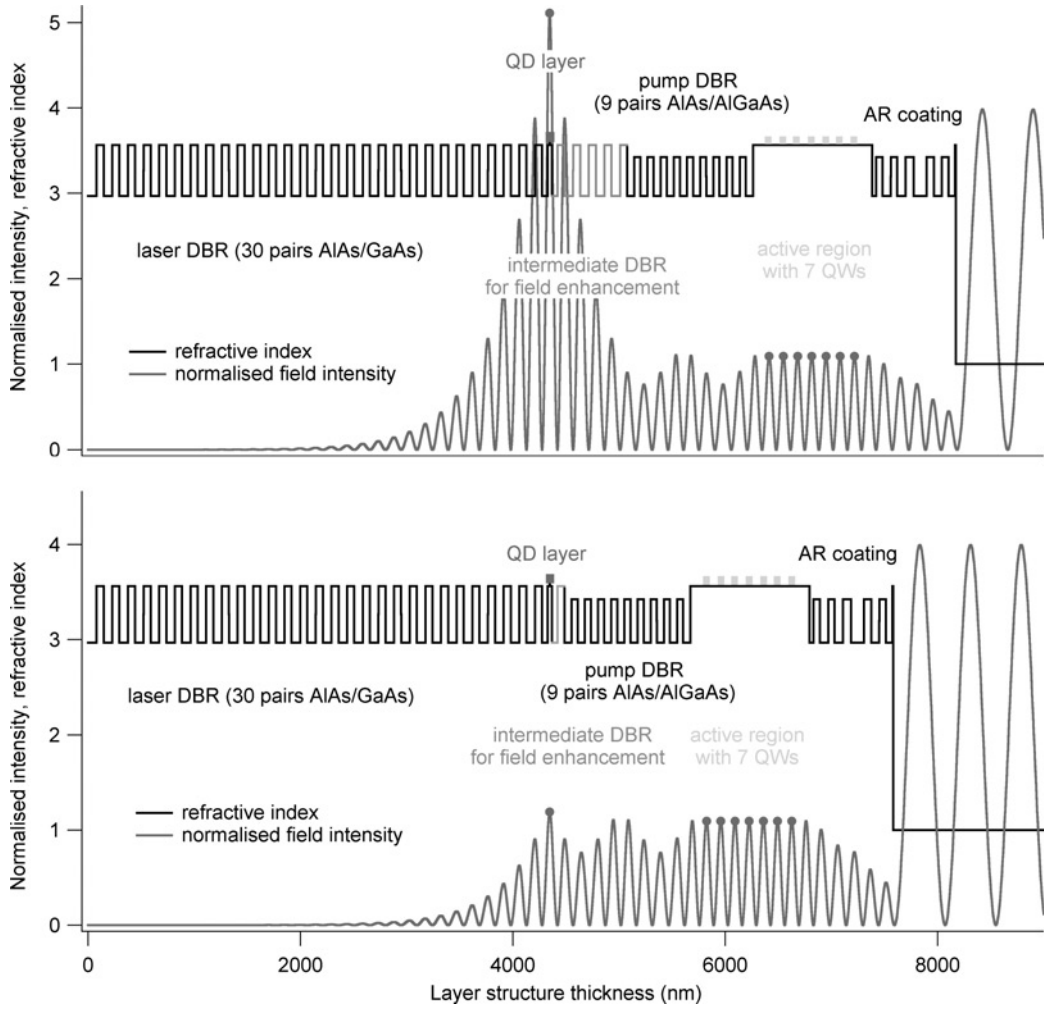

Figure 7 *Calculated normalised standing-wave intensity (grey) in a MIXSEL (normalised with respect to the incoming intensity which results just before the MIXSEL structure in a peak intensity of 4 assuming 100% reflectivity)*

The MIXSEL layer structure is shown with the refractive indices for the different layers (black)
The field enhancement in the absorber can be controlled by the number of layer pairs in the intermediate DBR
The top graph shows our current MIXSEL design with a five-pair intermediate DBR and below for a one-pair intermediate DBR

Such a growth error would reduce the gain and raise the modulation depth of the absorber by more than 50% that would prevent lasing. Hence, a careful calibration and control of the material fluxes during MBE growth is required.

As can be seen in Fig. 8*a*, the field enhancement for both in the QD absorber layer and the QW gain layers depend strongly on the wavelength. By selecting the operation wavelength, we can control their relative ratio, which gives us one adjustable parameter to optimise modelocking of the MIXSEL. We used an intracavity etalon with adjustable angle of incidence to tune the lasing wavelength. However, not only the relative field enhancement depends on the operation wavelength but also the dispersion. Strong wavelength dependent dispersion is introduced by the residual reflection from the AR coating and the lower high reflecting laser DBR, which form a Gires–Tournois interferometer (GTI) [41]. It is well known that such a GTI introduces strong group delay dispersion (GDD) as shown for the two different MIXSEL designs (Fig. 7). Dispersion control is important for modelocking of VECSELs [31]. To reduce the GDD we designed a top AR coating with ten numerically optimised layers for a maximum residual reflection of $\simeq$1% to obtain sufficiently small GDD as shown in Fig. 8*b*.

4 Modelocking results and power scaling

The MIXSEL wafer was cleaved in 5 × 5 mm pieces and a sample was soldered to a copper heat sink. It was then placed on a Peltier-cooled mount for temperature stabilisation. The first MIXSEL was tested in a straight cavity with a 60 mm-curved output coupler with 0.35% transmission (Fig. 9*a*). The structure was OP at an angle of 45° by a diode laser at 808 nm with a pump spot of 80 μm. A 25 μm silica etalon was placed inside the cavity for wavelength selection to adjust both intracavity GDD and the relative field enhancement in

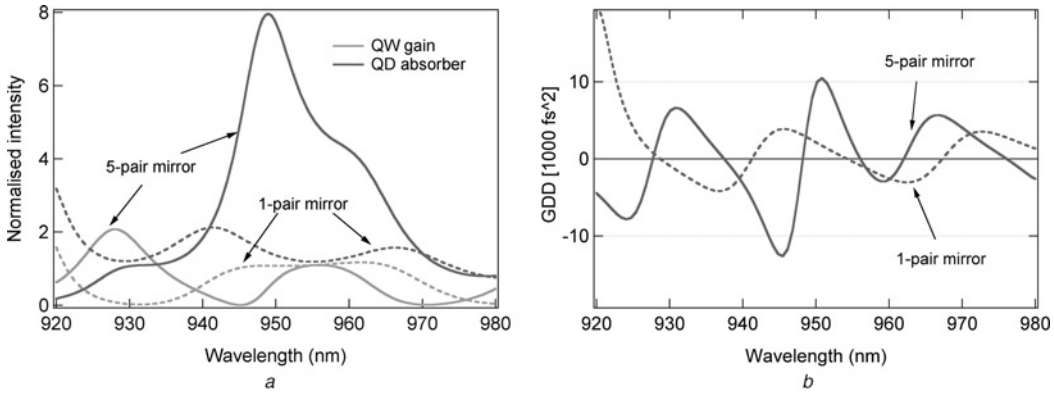

Figure 8 *Based on the MIXSEL design as shown in Fig. 7*

a Normalised intensity in the absorber and gain sections for a one-pair and five-pair intermediate mirror
b GDD for a one-pair and five-pair intermediate mirror

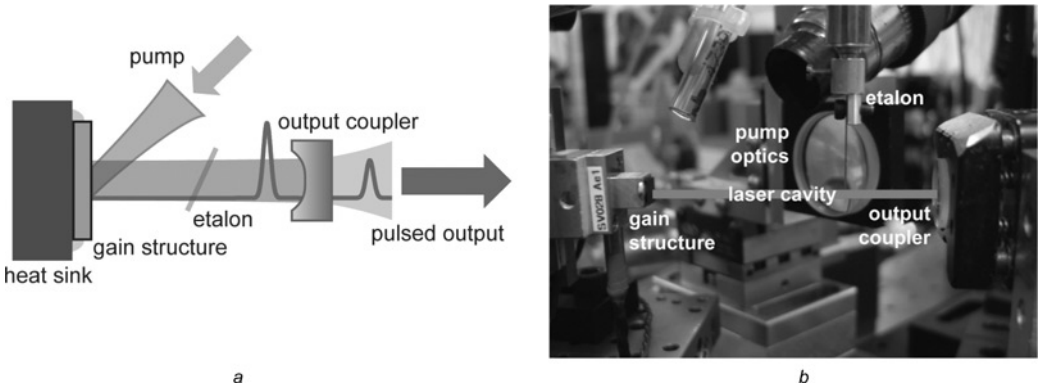

Figure 9 *MIXSEL cavity schematically and photo from experimental set-up: the laser resonator consists of the semiconductor structure and the external output coupler*

a Schematically experimental set-up
b Photo
The semiconductor structure is soldered to a heat sink and OP at an angle of 45°C
The etalon selects the lasing wavelength for stable modelocking operation

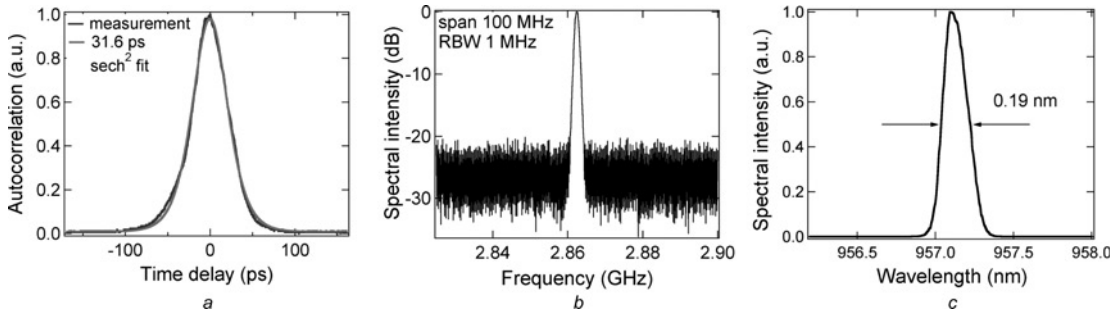

Figure 10 *Pulse characterisation of an OP MIXSEL with an average output power of 185 mW*

a Autocorrelation and sech2-fit for a 31.6 ps pulse (FWHM)
b Microwave spectrum on a 100 MHz span with 1 MHz resolution bandwidth
c Optical spectrum

absorber and gain (unfortunately not independently). Stable modelocking was obtained with 34.6 ps pulses at a wavelength of 953 nm. At this point, the average output power was limited to 40 mW at a pump power of 1.5 W [24], which was obtained at a heat sink temperature of −10°C. A roll-over was observed for higher pump power, which was attributed to thermal effects (no permanent damage was observed). Thermal roll-over is usually caused by

doi: 10.1049/iet-opt.2008.0038

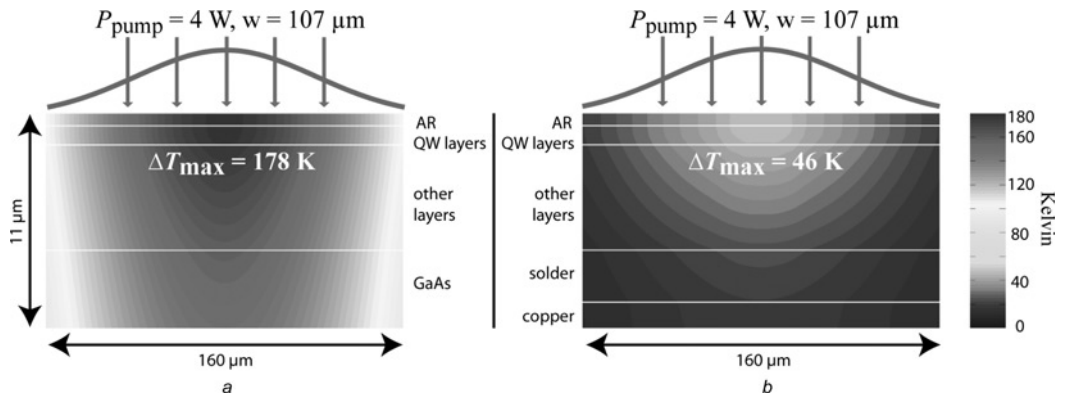

Figure 11 *Numerical simulation of the temperature increase in the semiconductor MIXSEL structure*

a 'right-side-up' MIXSEL with a 600 μm GaAs substrate
b 'upside-down' MIXSEL on a copper heat sink and without the GaAs substrate

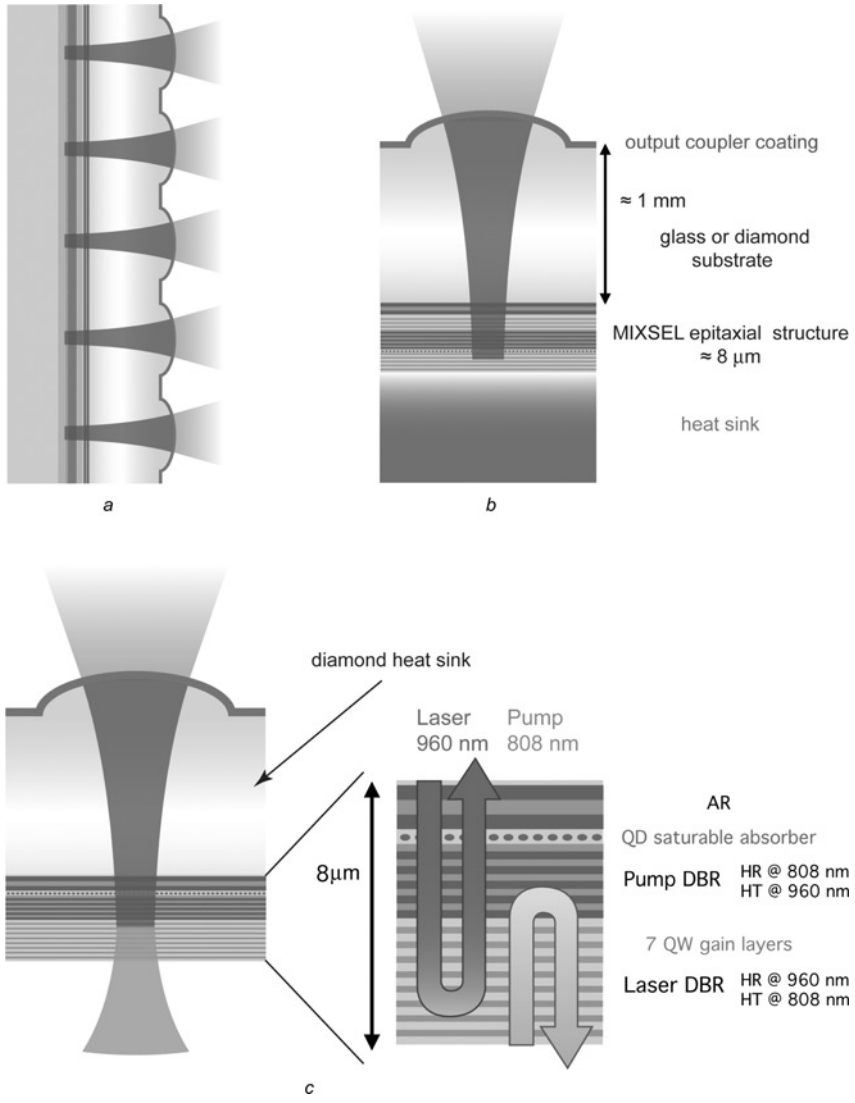

Figure 12 *Wafer-scale integration concept*

a Semiconductor MIXSEL structure wafer glued to a transparent wafer into which the curved output coupler is etched
b Wafer-based MIXSEL mounted onto a heat sink
Ideally suited for electrical pumping or integrated optical pumping
c Wafer-based MIXSEL for backside optical pumping when transparent external cavity wafer is also used as a heat sink (for example with diamond)

temperature gradients and/or the absolute temperature increase. Transverse temperature gradient can lead to thermal lensing and aberrations, which destabilise the cavity mode. In our case, we attributed the roll-over to the gain reduction because of the absolute temperature increase. The thermal wavelength shift of the peak gain emission is ~0.3 nm per Kelvin. As explained above, the lasing wavelength is controlled with an intracavity etalon, such that an optimum relative field enhancement between QD and QW region is achieved. When the temperature increases, the QW gain peak shifts and the gain at the correct wavelength for optimum field enhancement is reduced.

We simulated the temperature increase in the structure using a finite element method: for a pump spot of 80 μm and 1.5 W of pump power, we obtained a temperature increase of more than 110 K compared with the heat sink temperature, which resulted in a temperature of 100°C inside the MIXSEL. This corresponded to a wavelength shift of ~30 nm. To confirm that the temperature increase was the main limiting factor, we cooled the heat sink further down to −50°C and increased the pump power. We optimised the set-up with a larger pump spot of 110 μm and an output coupler with 0.7% transmission (Fig. 9*b*), and we indeed observed stable modelocked operation with 185 mW average output power and 31.6 ps long pulses at 957 nm (Fig. 10). The cavity was 52.4 mm long, corresponding to a pulse repetition rate of 2.86 GHz. The average output power was increased by a factor of 4 compared with the previous results [24]. The result was limited by the maximum pump power available in our setup (4 W).

The simulation of the thermal properties predicts an increase of 180 K at the centre of the pump spot, which corresponds to a maximum temperature of 130°C inside the MIXSEL structure (Fig. 11). Numerical simulations show that the temperature increase can be reduced to 46 K at the same pump power for an 'upside-down' MIXSEL, that is soldered onto a copper substrate with the GaAs substrate etched away. We expect that such an OP-MIXSEL will achieve power levels of several watts (similar to the previously demonstrated SESAM-modelocked VECSELs). Further optimisation of the integrated QD absorber and better growth accuracy should reduce the pulse duration to a few picoseconds, as was already demonstrated with QD-SESAMs in a 1 : 1 modelocking set-up [39].

5 Conclusion and outlook

In this paper, we presented a complete description of the vertical integration of a gain and absorber in a single semiconductor structure, the MIXSEL. Such a modelocked laser is compact, robust and has the potential for cost-efficient wafer-scale high volume manufacturing. A possible design concept is shown in Fig. 12. A transparent wafer into which the curved output couplers are etched is contacted directly onto the MIXSEL semiconductor structure (Figs. 12*a* and 12*b*). Note this figure is not to scale, the thickness of the semiconductor is strongly enlarged and the pulse mostly propagates in the transparent wafer. The thickness of the semiconductor structure is only ≃10 μm, which is small compared with the total optical cavity length (about 3 mm in the case of a 50 GHz MIXSEL). The finished wafer structure as shown in Fig. 12*a* can then be diced into individual MIXSELs (Fig. 12*b*). The method appears very promising, especially when combined with electrical pumping or integrated optical pumping [42]. But this approach appears also well suited for OP-MIXSELs. The MIXSEL can also be OP from the back after the GaAs substrate has been removed Fig. 12*c*. In this case, the transparent wafer would also act as the heat sink. With its simple straight cavity configuration, the MIXSEL has the potential for adjustable multi-10 GHz repetitions rates.

The MIXSEL presented here, generates pulses at 2.86 GHz with an average output power of 185 mW. Further optimisation of the QD saturable absorber inside the MIXSEL structure should lead to shorter transform-limited pulses in the few picosecond regime. A stronger field enhancement in the absorber would also support QD gain material, which has the potential for a broader gain bandwidth because of inhomogeneous broadening. This relaxes the requirements on the saturable absorber recovery time and modulation depth and therefore could more easily support femtosecond pulses.

6 Acknowledgment

This work was supported in part by the Intel Corporation through a university sponsored research agreement, the European Network of Excellence ePIXnet, the European FP7 Collaborative Project FAST-DOT, and ETH Zurich with the FIRST clean-room facility.

7 References

[1] KELLER U.: 'Recent developments in compact ultrafast lasers', *Nature*, 2003, **424**, pp. 831–838

[2] TAGA H., SUZUKI M., NAMIHIRA Y.: 'Polarization mode dispersion tolerance of 10 Gbit/s NRZ and RZ optical signals', *Electron. Lett.*, 1998, **34**, pp. 2098–2100

[3] MOLLENAUER L.F., MAMYSHEV P.V.: 'Massive wavelength-division multiplexing with solitons', *IEEE J. Quantum Electron.*, 1998, **34**, pp. 2089–2102

[4] KOBRINSKY M.J.: 'On-chip optical interconnects', *Intel Technol. J.*, 2004, **8**, (2)

doi: 10.1049/iet-opt.2008.0038

[5] HUANG D., SWANSON E.A., LIN C.P. *ET AL.*: 'Optical coherence tomography', *Science*, 1991, **254**, pp. 1178–1181

[6] FUJIMOTO J.G.: 'Optical coherence tomography', *C. R. Acad. Sci., Ser. IV*, 2001, **2**, pp. 1099–1111

[7] DENK W., STRICKLER J.H., WEBB W.W.: 'Two-photon laser scanning fluorescence microscopy', *Science*, 1990, **248**, pp. 73–76

[8] TELLE H.R., STEINMEYER G., DUNLOP A.E., STENGER J., SUTTER D.H., KELLER U.: 'Carrier-envelope offset phase control: a novel concept for absolute optical frequency measurement and ultrashort pulse generation', *Appl. Phys. B*, 1999, **69**, pp. 327–332

[9] HOLZWARTH R., UDEM T., HÄNSCH T.W., KNIGHT J.C., WADSWORTH W.J., RUSSELL P.S.J.: 'Optical frequency synthesizer for precision spectroscopy', *Phys. Rev. Lett.*, 2000, **85**, pp. 2264–2267

[10] HOLZWARTH R., ZIMMERMANN M., UDEM T., HÄNSCH T.W.: 'Optical clockworks and the measurement of laser frequencies with a mode-locked frequency comb', *IEEE J. Quantum Electron.*, 2001, **37**, pp. 1493–1501

[11] STENGER J., BINNEWIES T., WILPERS G. *ET AL.*: 'Phase-coherent frequency measurement of the Ca intercombination line at 657 nm with a Kerr-lens mode-locked femtosecond laser', *Phys. Rev. A*, 2001, **63**, p. 021802-01-04

[12] KUZNETSOV M., HAKIMI F., SPRAGUE R., MOORADIAN A.: 'High-power ($>$0.5-W CW) diode-pumped vertical-external-cavity surface-emitting semiconductor lasers with circular TEM_{00} beams', *IEEE Photon. Technol. Lett.*, 1997, **9**, pp. 1063–1065

[13] TROPPER A.C., HOOGLAND S.: 'Extended cavity surface-emitting semiconductor lasers', *Quantum Electron.*, 2006, **30**, pp. 1–43

[14] LEE J., LEE S., KIM T., PARK Y.: '7 W high-efficiency continuous-wave green light generation by intracavity frequency doubling of an end-pumped vertical external-cavity surface emitting semiconductor laser', *Appl. Phys. Lett.*, 2006, **89**, pp. 241107–1–3

[15] KREUTER P., WITZIGMANN B., MAAS D.J.H.C., BARBARIN Y., SÜDMEYER T., KELLER U.: 'On the design of electrically-pumped vertical-external-cavity surface-emitting lasers', *Appl. Phys. B*, 2008, **91**, (2), pp. 257–264

[16] MCINERNEY J.G., MOORADIAN A., LEWIS A. *ET AL.*: 'High-power surface emitting semiconductor laser with extended vertical compound cavity', *Electron. Lett.*, 2003, **39**, pp. 523–525

[17] CHILLA J., BUTTERWORTH S., ZEITSCHEL A. *ET AL.*: 'High power optically pumped semiconductor lasers', presented at Photonics West 2004, Solid State Lasers XIII: Technology and Devices, Proc. SPIE 5332, 2004

[18] RUDIN B., MAAS D.J.H.C., BELLANCOURT A.R., SÜDMEYER T., GINI E., KELLER U.: 'Efficient high-power VECSEL generates 20 W continuous-wave radiation in a fundamental transverse mode', presented at EPS-QEOD Europhoton Conf., Paris, (France), 2008

[19] HOOGLAND S., DHANJAL S., TROPPER A.C. *ET AL.*: 'Passively mode-locked diode-pumped surface-emitting semiconductor laser', *IEEE Photon. Technol. Lett.*, 2000, **12**, pp. 1135–1138

[20] KELLER U., WEINGARTEN K.J., KÄRTNER F.X. *ET AL.*: 'Semiconductor saturable absorber mirrors (SESAMs) for femtosecond to nanosecond pulse generation in solid-state lasers', *IEEE J. Sel. Top. Quantum*, 1996, **2**, pp. 435–453

[21] GARNACHE A., HOOGLAND S., TROPPER A.C., SAGNES I., SAINT-GIRONS G., ROBERTS J.S.: '$<$500-fs soliton pulse in a passively mode-locked broadband surface-emitting laser with 100-mW average power', *Appl. Phys. Lett.*, 2002, **80**, pp. 3892–3894

[22] KLOPP P., SAAS F., ZORN M., WEYERS M., GRIEBNER U.: '290-fs pulses from a semiconductor disk laser', *Opt. Express*, 2008, **16**, pp. 5770–5775

[23] KELLER U., TROPPER A.C.: 'Passively modelocked surface-emitting semiconductor lasers', *Phys. Rep.*, 2006, **429**, pp. 67–120

[24] MAAS D.J.H.C., BELLANCOURT A.-R., RUDIN B. *ET AL.*: 'Vertical integration of ultrafast semiconductor lasers', *Appl. Phys. B*, 2007, **88**, pp. 493–497

[25] HÄRING R., PASCHOTTA R., ASCHWANDEN A., GINI E., MORIER-GENOUD F., KELLER U.: 'High-power passively mode-locked semiconductor lasers', *IEEE J. Quantum Electron.*, 2002, **38**, pp. 1268–1275

[26] ALFORD W.J., RAYMOND T.D., ALLERMAN A.A.: 'High power and good beam quality at 980 nm from a vertical external-cavity surface-emitting laser', *J. Opt. Soc. Am. B*, 2002, **19**, pp. 663–666

[27] HAIML M., SIEGNER U., MORIER-GENOUD F. *ET AL.*: 'Optical nonlinearity in low-temperature-grown GaAs: microscopic limitations and optimization strategies', *Appl. Phys. Lett.*, 1999, **74**, pp. 3134–3136

[28] MAAS D.J.H.C., RUDIN B., BELLANCOURT A.-R. *ET AL.*: 'High precision optical characterization of semiconductor saturable absorber mirrors', *Opt. Express*, 2008, **16**, pp. 7571–7579

[29] HAIML M., GRANGE R., KELLER U.: 'Optical characterization of semiconductor saturable absorbers', *Appl. Phys. B*, 2004, **79**, pp. 331–339

[30] SIEGMAN A.E.: 'Lasers: university science books' (Mill Valley, California, 1986)

[31] PASCHOTTA R., HÄRING R., KELLER U., GARNACHE A., HOOGLAND S., TROPPER A.C.: 'Soliton-like pulse formation mechanism in passively mode-locked surface-emitting semiconductor lasers', *Appl. Phys. B*, 2002, **75**, pp. 445–451

[32] SPÜHLER G.J., GRANGE R., KRAINER L. *ET AL.*: 'Semiconductor saturable absorber mirror structures with low saturation fluence', *Appl. Phys. B*, 2005, **81**, pp. 27–32

[33] KIRSTAEDTER N., LEDENTSOV N.N., GRUNDMANN M. *ET AL.*: 'Low threshold, large T injection laser emission from (InGa)As quantum dots', *Electron. Lett.*, 1994, **30**, pp. 1416–1417

[34] GERMANN T.D., STRITTMATTER A., POHL J. *ET AL.*: 'High-power semiconductor disk laser based on InAs/GaAs submonolayer quantum dots', *Appl. Phys. Lett.*, 2008, **92**, pp. 101–123

[35] GARNACHE A., HOOGLAND S., TROPPER A.C., GERARD J.M., THIERRY-MIEG V., ROBERTS J.S.: 'CLEO/Europe-EQEC', 2001

[36] RAFAILOV E.U., WHITE S.J., LAGATSKY A.A. *ET AL.*: 'Fast quantum-dot saturable absorber for passive mode-locking of solid-state lasers', *IEEE Photon. Technol. Lett.*, 2004, **16**, pp. 2439–2441

[37] RAFAILOV E.U., CATALUNA M.A., SIBBETT W.: 'Mode-locked quantum-dot lasers', *Nature Photon.*, 2007, **1**, pp. 395–401

[38] LORENSER D., UNOLD H.J., MAAS D.J.H.C. *ET AL.*: 'Towards wafer-scale integration of high repetition rate passively mode-locked surface-emitting semiconductor lasers', *Appl. Phys. B*, 2004, **79**, pp. 927–932

[39] LORENSER D., MAAS D.J.H.C., UNOLD H.J. *ET AL.*: '50-GHz passively mode-locked surface-emitting semiconductor laser with 100 mW average output power', *IEEE J. Quantum Electron.*, 2006, **42**, (7–8), pp. 838–847

[40] MALIK S., ROBERTS C., MURRAY R., PATE M.: 'Tuning self-assembled InAs quantum dots by rapid thermal annealing', *Appl. Phys. Lett.*, 1997, **71**, pp. 1987–1989

[41] GIRES F., TOURNOIS P.: 'Interferometre utilisable pour la compression d'impulsions lumineuses modulees en frequence', *C. R. Acad. Sci.*, 1964, **258**, pp. 6112–6115

[42] ILLEK S., ALBRECHT T., BRICK P. *ET AL.*: 'Vertical-external-cavity surface-emitting laser with monolithically integrated pump lasers', *IEEE Photon. Technol. Lett.*, 2007, **19**, pp. 1952–1954

doi: 10.1049/iet-opt.2008.0038